Control of a 2.4MW Linear Synchronous Motor for launching roller-coasters

A. Veltman(1,2), P. van der Hulst (2), M.C.P. Jonker(3), J.P. van Gurp(3)
(1) Eindhoven Univertsity of Techn., P.O. Box 513, 5600 MB Eindhoven, Netherlands.
(2) Piak Electronic Design b.v., Markt 49, 4101 BW Culemborg, the Netherlands.
t: +31-345-534126, f: +31-345-534127, www.piak.nl
(3) GTI Electroproject b.v., P.O. Box 441, 1500 EK Zaandam, the Netherlands.
t :+31756811111, www.electroproject.nl
Author Information : a.veltman@piak.nl

Keywords

LSM, current control, sensor-less control, switched stators

Abstract

To accelerate a heavy roller-coaster train to a speed of 25m/s in less than 3 seconds requires a lot of thrust. A 2.4MW Linear Synchronous Motor is applied for this function. Optimal thrust implies optimal current control. Because of the increasing velocity along the track, the stator configuration changes continuously during a launch (sequentially switched stator). A strategy to control 3kA of current during abrupt changes in stator inductance, while maintaining thrust, is presented.

1 System configuration

A 2.4 MW Linear Synchronous Motor (LSM) is used to accelerate a roller-coaster train from standstill to a final speed of 25m/s within a travelled distance of about 40m in a little less than 3 seconds. Initial acceleration is about 1.5g. The acceleration reduces beyond the velocity of maximum power, yielding an economic constant power operation for the main part of the launch.

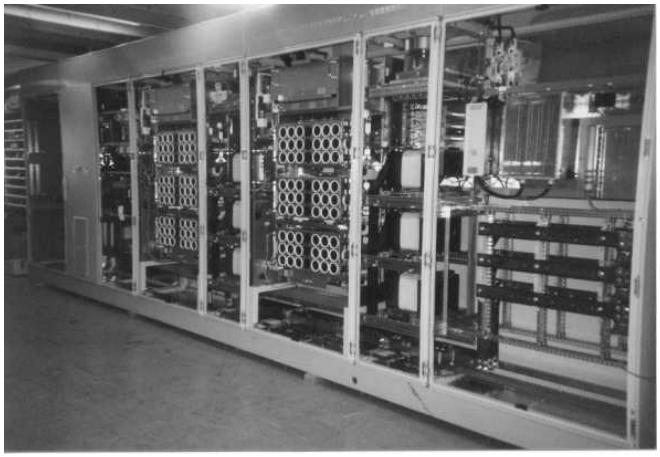

Figure 1 2.4MW inverter under construction

The LSM is of the long-stator type. It consists of wound stators mounted on the track (the stator) with a length of about 60m. Permanent magnets are mounted on the pusher-car that pushes the roller-coaster train from underneath. After the pusher-car reaches the required speed of 25m/s, the train continues in a passive fashion, leaving the pusher-car behind. The 6m long pusher-car decelerates to standstill in about 1 second and then returns to the starting position to launch the next train.

The long stator is fed by a group of parallel inverters able to deliver 2.4MW using a 1000V DC-link voltage. The developed current controller drives the gate signals of the IGBT's in a direct fashion. The standard modulators in the inverter are not used.

In order to waste as little voltage as possible, the long stator is divided into sections with a length of 3 meters each, all connected in series. Each of the sections can be shorted by means of heavy-duty thyristors. By shorting all sections except the 3 (partly) covered by the magnets of the pusher-car, inductance and resistance are minimised. Sections are shorted after the pusher-car has passed and 'opened' just before the pusher-car enters a new section. Since all stator sections are different to allow optimal constant power operation, large abrupt (asymmetric) steps in inductance and resistance occur. The equivalent circuit in fig. 5 shows all relevant electrical components. The voltage U_s represents the inverter voltage of all three inverters in parallel, L_r represents the coupling inductors to allow

paralleled inverters to share current. The effective inductance *L(thy)* depends on the status of the thyristor switches as does the effective stator resistance R_s.

Figure 2 Accelerating pusher-car without train.

These large parameter changes occur abruptly in a step-wise fashion and make precise control of the motor current (up to 3kA) a challenge. A system based on Hall sensors is used for position measurement, the set-point for the current vector is based on the actual position, velocity and acceleration. We are presently working on a sensor-less position estimator: first results in figures 6 and 7. Figure 1 shows the inside of the power converter under construction, figure 3 depicts the test track of the LSM launch system with thyristor switch boxes adjacent to the track. Figure 4 shows the construction of the stator with two-sided NeFeB magnets and airgaps of approximately 1cm.

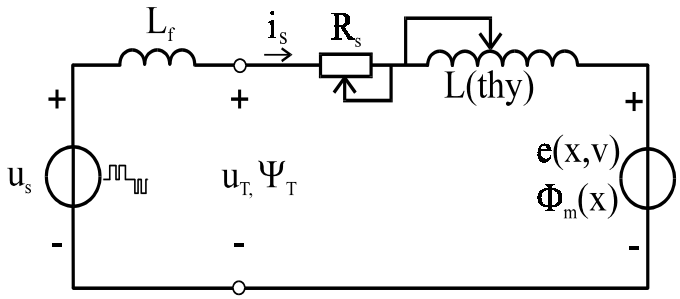

Figure 5 Simplified equivalent per phase circuit of LSM with switched stator.

Figure 3 Test track of LSM, stators and guiding fin are visible. Pusher-car is underneath the train. Thyristors in boxes on left side.

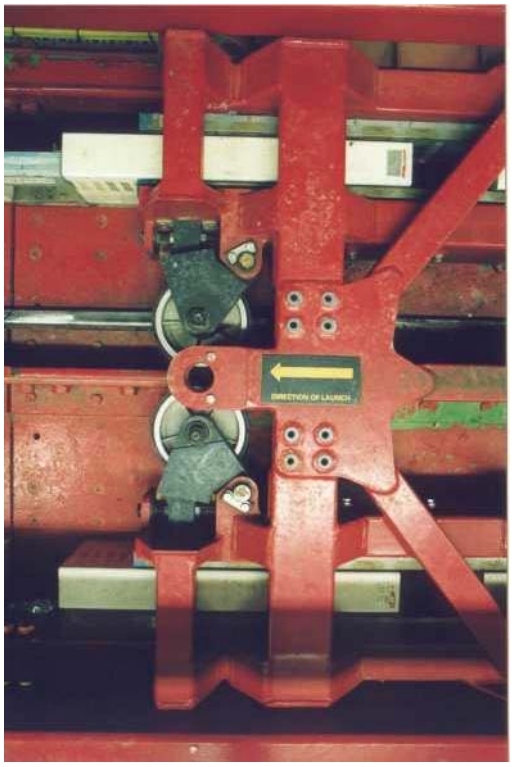

Figure 4 Magnet-stator-magnet sandwich on either side of pusher-car, vertical guide-rail in centre.

Figure 2 shows an accelerating pusher-car in the final set-up. Figures 6 and 7 show a close-up measurement of a launched train.

2 Synchronous frame hysteresis controller

Requirements for the motor current controller are:

1. Smooth thrust during fast acceleration.
2. Accurate current control during switching of thyristors: unbalanced load and stepwise parameter changes.
3. Keep current when maximum voltage is reached.
4. Use low switching frequency (max 1kHz at 3kA)
5. Minimise acoustic noise

Since most conventional current controllers are based on a motor model with constant parameters, these goals are hard to achieve. Requirements 2 and 4 seem to contradict each other since fast control needs high bandwidth and thus a high switching frequency.
The presented synchronous-frame hysteresis controller does show excellent dynamics, even at low switching frequencies (see figures 6 and 7). A hysteresis current controller is inherently insensitive to parameter variations, and generates a more random-noise-like acoustic spectrum than carrier-based PWM modulators. The relations between voltage, its mathematical integral flux, and current that are present in the equivalent circuit in figure 5 are explained in figure 8.

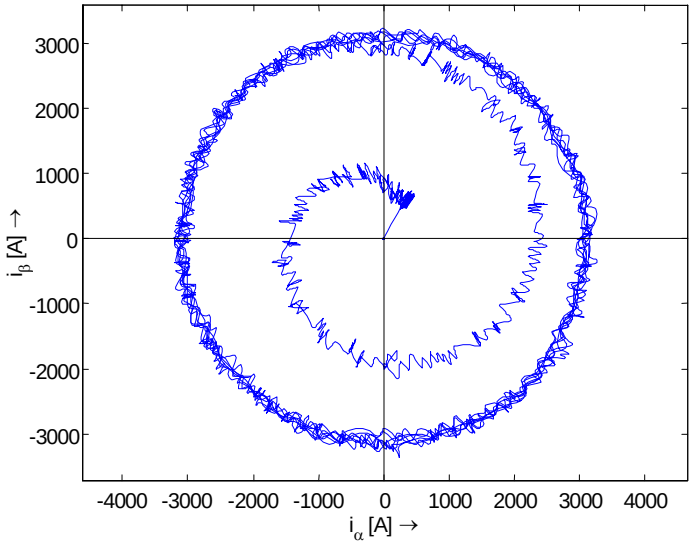

Figure 6 Measured data: current vector during launch in first second, sensor-less position estimation

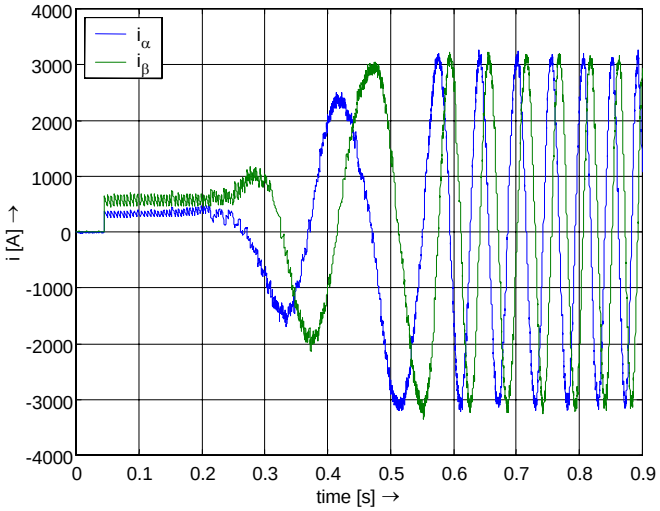

Figure 7 Measured data: start of launch with controlled build up to 2200A, sensor-less position.

The prime goal of the current controller is to realize a required value of i_q^* within the given constraints of the inverter. The output voltage of the three phase inverter can be regarded as one of 2^3=8 possible states, of which six are called 'active vectors' and two (000 and 111) are called 'zero vectors', see figure 8(c). The current controller makes a kind of pulse width modulated output such that the required current is realized as quickly as possible by means of only four switching rules as shown in figure 8(b). The strategy is straightforward: when the difference between reference and actual current value is within the gray box, the present state of the inverter is maintained until one of the boundaries is crossed. Each of the boundaries has a distinct effect on the switching state. Suppose the inverter state is 110 (active vector at 60°, see figure 8(c)). A stop would mean switching to the nearest zero vector which is 111. A stop causes a zero voltage on the motor terminals, hence the integral of voltage, the terminal flux Ψ_T will hold position. A +60° transition would imply going to 010 and a -60° transition would imply going to 100, since voltage represents the direction of increase of the flux Ψ_T, the flux orbit as seen in figure 8(a) gets an additional corner. All other active vectors

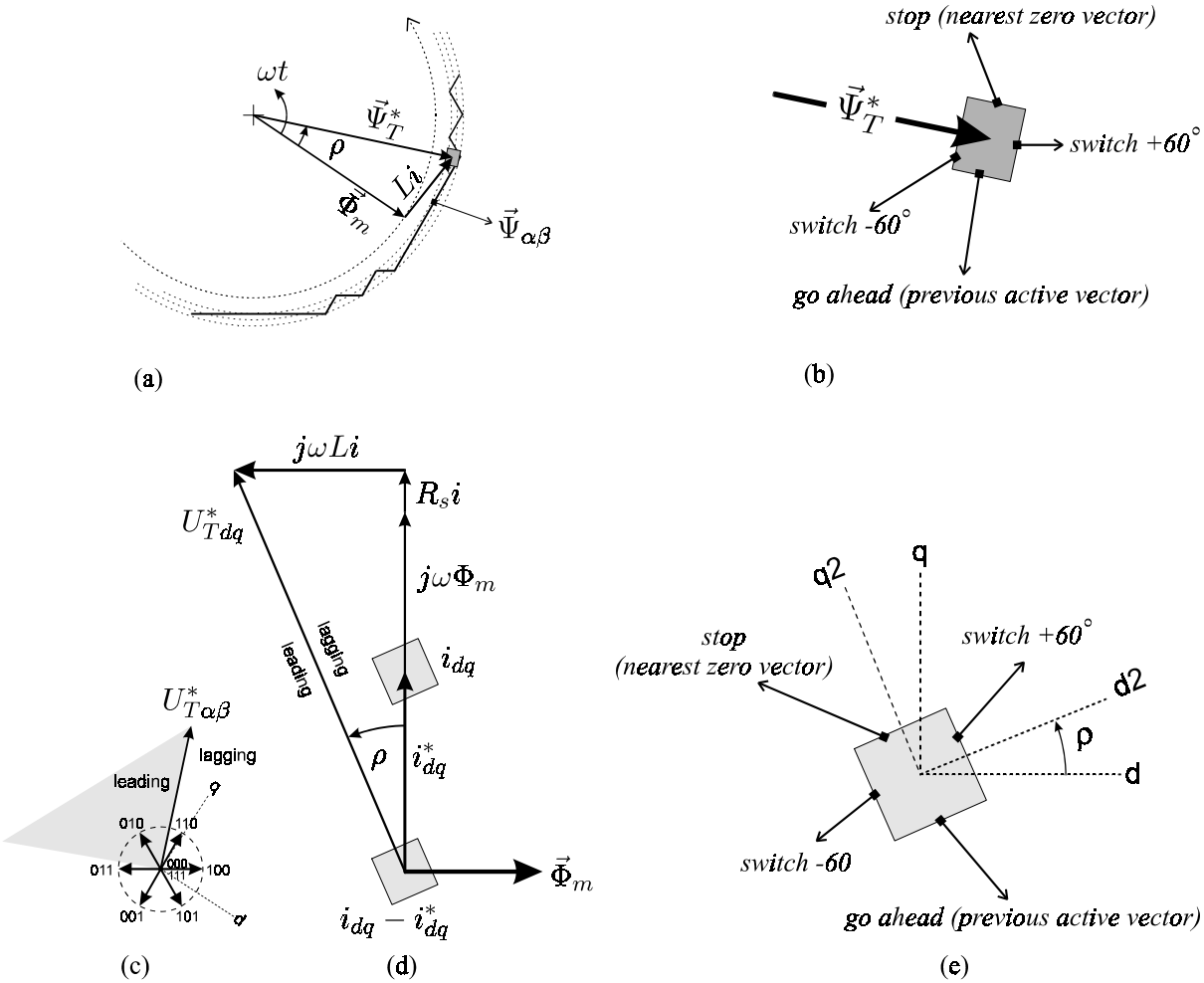

Figure 8 Asynchronous current control switching algorithm. (a) The switching box is aligned with the mean stator flux. (b) Switching actions on crossing boundaries when assuming a reference for terminal flux. (c) Definition of voltage vectors, mean terminal voltage vector and leading/lagging. (d) Vector representation of voltages and current in synchronous motor operating at load angle ρ. (e) Load angle correction of error box.

also have their own adjacent states that can be regarded as a +60°, a -60° and a zero vector. It is evident that each boundary transition involves the change of only one phase, which makes this strategy effective.

2.1 A 2-dimensional hysteresis controller

The voltage needed to realize i_q^* depends mainly on the velocity of the pusher-car, the total coupled magnetic flux (depending on the number of active turns) and the present inductance. The latter two strongly depend on the position on the launch track and the status of the thyristor switches along the track respectively (also see figure 3).

The required inverter flux to generate i_q^* is depicted in figure 8(a). The flux across the inductance equals $L \cdot i$ and the current is perpendicular to the magnet flux Φ_m, here the flux across the resistance R_s is neglected for clarity. The terminal flux $\vec{\Psi}_T^*$ is leading the magnet flux by angle ρ The best way to orient the switching box is to align it to $\vec{\Psi}_T^*$. However, this flux is not known, because the inductance L is not known to the current controller at every instant.

figure 8(b) shows the best orientation. figure 8(d) is the same situation but seen from the voltage point of view. The Electro-motive force (emf) $j\omega\Phi_m$ is leading Φ_m by 90°. To achieve maximum force per ampère, i_q^* is parallel to the emf. The voltage drop in resistance $R_s\, i$ is also parallel to the emf. The voltage over series inductance L is leading the current by 90°, causing the required terminal voltage U_{Tdq}^* to lead the current by load-angle ρ. Load angle ρ can be estimated in various ways, and should be done with sufficient bandwidth to allow following fast impedance changes.

2.2 Implicit alignment to $\vec{U}_T$

As set points we use i_q^* and i_d^*. As discussed above, we will for now assume that $i_d^* = 0$. In case there is insufficient DC link voltage to realize i_q^*, a negative value of i_d^* can buy force at the expense of more stator losses as is shown in figure 9.
With the measured $\vec{i}_{dq}$ two error values can be distinguished, (see figure 8(d)):

$$\begin{aligned} \Delta i_d &= i_{Td} - i_d^* \\ \Delta i_q &= i_{Tq} - i_q^* \end{aligned} \tag{1}$$

By using an estimate of load-angle ρ, the switching rules can be applied to a transformation of $\Delta\vec{i}_{dq}$ according to:

$$\Delta\vec{i}_{dq2} = \begin{pmatrix} \Delta i_{d2} \\ \Delta i_{q2} \end{pmatrix} = \begin{bmatrix} \cos\rho & \sin\rho \\ -\sin\rho & \cos\rho \end{bmatrix} \cdot \begin{pmatrix} \Delta i_d \\ \Delta i_q \end{pmatrix} \tag{2}$$

By applying the switching rules in figure 8(b) to the transformed error vector $\Delta\vec{i}_{dq2}$, an excellent switching behavior results. Experimental results are shown in various graphs in following sections.

2.2.1 Handling Voltage shortage

Conventional hysteresis controllers are usually of the per-phase type with problems of limit cycles (see [1]). The presented current controller uses a 2 dimensional vector approach with two criteria: one for amplitude, one for angle as shown in figure 8(b,c). The robustness of this approach is depicted in figures 6, 7 and 10. Figure 7 shows the very low switching frequency during the start of the train, figure 6 shows the control of the current-vector in a stationary α and β reference frame. An interesting detail can be seen in figure 10 where the inductance reduces by a large amount at t=1.042s, as a consequence the switching frequency goes up, but the current vector is not noticeably affected. Note that the inductance change of one of the delta connected phases reduces from 1.1mH to 0.73mH within a few milliseconds. The apparent inductance change on the inverter terminals is 1/3 of this value (Δ-Y equivalent), hence the flux change involved here is $\Delta\Psi = i \cdot \Delta L / 3$. The switching rules realize this mutual amplitude and phase change of the terminal flux by directly shortening the time of active vectors, which causes an increase in switching frequency [3].

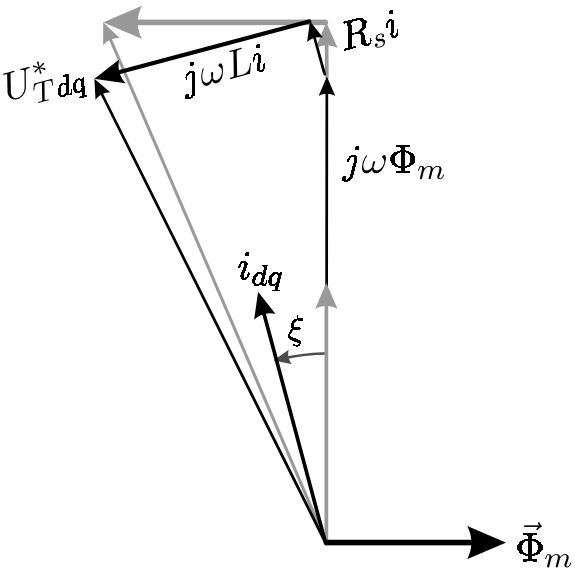

Figure 9 Introducing negative i_d to reduce required voltage.

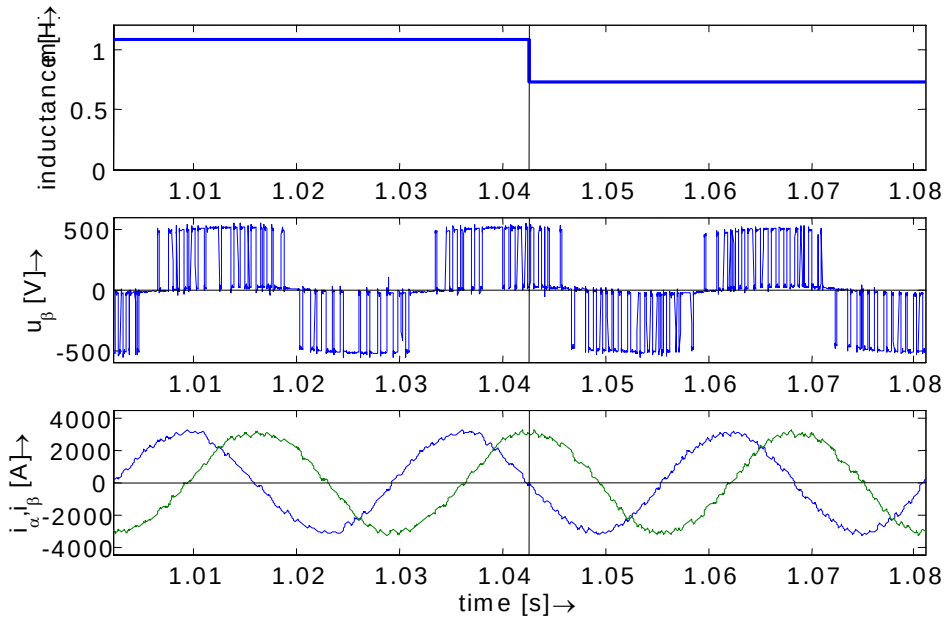

Figure 10 Measured data: stepwise change in inductance, switching frequency increases, current shape unaffected.

3 Roller-coaster performance

During a launch cycle, various stages can be distinguised. A full cycle is depicted in figure 11. A cycle starts at a postion of about 6m. To avoid 'whip-lash' risk of the passengers on board, the launch consists of a gradual increase of the thrust, as shown in figure 12. During the thrust build up, the displacement of the train is about 0.2m. Figure 11 shows that speed increases rapidly in the first meters of the track: after 4m of travelled distance, the speed already crosses 10m/s. The remaining 45m are needed to accelerate further from 10m/s to 25m/s. Once the required speed is reached, the current is reduced to zero and the pushercar soon enters the eddy-current brakes between 60m and 75m. Figure 11 shows that the realized current level is slightly reduced due to lack of voltage between 45 and 55m. In the eddy current brakes the decelleration is large, between –20 and -30m/s^2, causing the pushercar alone to stop within one second. The train with the passengers continues at a speed of 25m/s for some meters before it enters the first high looping of the complex curved ride. After delivering the train at the requircd speed, the pushercar decelerates in eddy current brakes and returns to the starting postion before engaging with the next train.

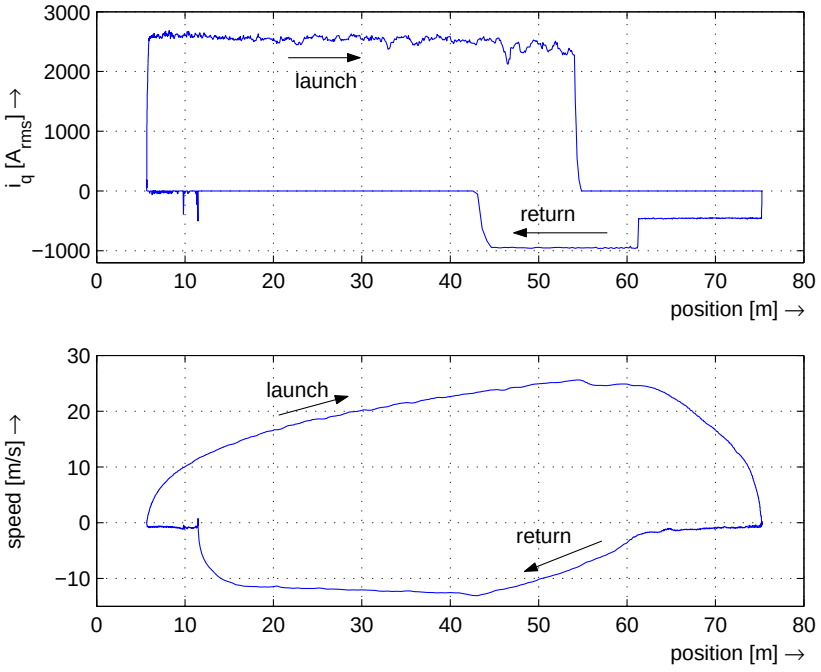

Figure 11 Current and pushercar speed versus position during one cycle. Cycle consists of start, launch with train, brake without train, slow return through eddy current brakes and fast return to initial position.

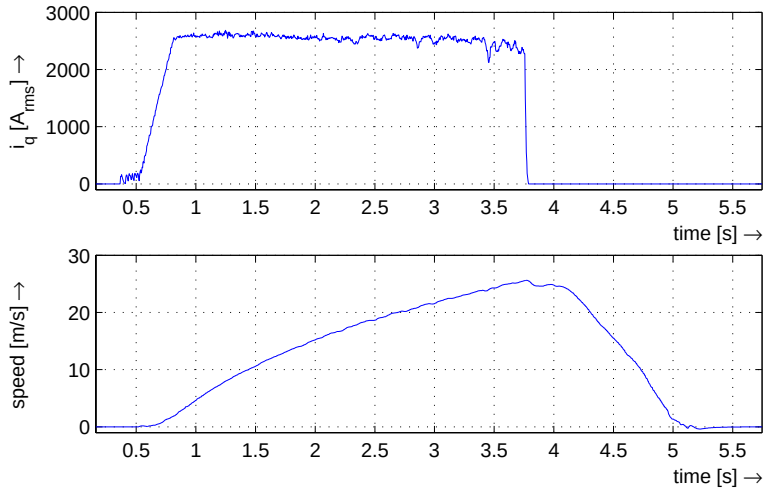

Figure 12 Launch with train to 25m/s. Current and speed versus time.

The return thru the eddy current brakes should be done at low speed to reduce excessive stator heating. After the brakes are passed, the acelleration is increased until the speed of 12m/s is reached, the rest of the return between 45m and 12m is in free wheeling mode. Mechanical brakes stop the pushercar on the return to base movement.

Both high speed and low speed pushercar braking were tested succesfully in various experiments. During these experiments additional brake choppers were placed on the DC link of the inverter to allow burning over 1.2MW of regenerative power. The proposed current control method proved well capable of full four quadrant operation. For safety reasons the practical roller coasters still use passive braking. Mechanical wear of pneumatic brakes could be reduced when active braking would be implemented. However, during the design of the present track layout, active braking was not considered. A more economic launch track design might be possible when including the possibility of high power active braking.

4 Conclusions

- An effective and robust current control strategy for a 2.4MW synchronous linear motor has been designed and implemented, needing no actual motor parameters such as inductance. The method allows controlling current straight thru step-wise inductance changes as do occur in switched-stator linear motors (at 3m intervals in this case, yielding 25/3=8.3 inductance changes per second at top speed).

Figure 13 Final result.

- The proposed current control strategy allows very low asynchronous switching frequencies (between 500Hz and 1000Hz) to control large currents of up to 3kA at high acceleration (up to 75Hz/s) with high phase accuracy.
- Active braking of up to 1.2MW has been succesfully tested, hence yielding full 4-quadrant capability when a sufficient brake chopper is installed.
- A sensorless position estimation strategy [4] was succesfully tested on the long LSM, using just measured voltages and currents of the inverter.
- The proposed current control makes it possible to repeatedly launch roller coaster trains up to 15m/s^2, 0…90km/h in 3s, using low cycle times, with only local forced air cooling.

5 References

1. D.M Brod, D.W. Novotny, 'Current control of VSI-PWM inverters', IEEE Trans. Ind. Appl., IA-21, 1985.
2. G.W McLean, 'Review of recent progress in linear motors', IEE proceedings Vol. 135, Nov. 1988
3. A.Veltman, 'The Fish Method : Interaction between AC-Machines and Switching Power Converters', Phd thesis, Delft University of Technology the Netherlands, 1994, ISBN 90-9006763-9
4. A.Veltman, 'A method and a device for sensorless estimating the relative angular position of the rotor of a three-phase synchronous motor', Patent application, EP1162106, 2001-12-12.